

Exploration of organic-inorganic hybrid perovskites for surface-enhanced infrared spectroscopy of small molecules

Jia Chen,^a Zhi-Hong Mo,^{*ab} Xiao Yang,^a Hai-Ling Zhou,^a Qin Gao^a

Chemicals and materials

PbI₂ (98%, Aladdin), methylamine (CH₃NH₂, 33% in methyl alcohol, Aladdin), hydriodic acid (HI, 47%, Aladdin), N-dimethylformamide (DMF, analytical grade, Aladdin), toluene (analytical grade, H₂O content 0.018%, Beijing Ouhe Technology Co. Ltd, China), and poly(methyl methacrylate) (PMMA, Aladdin) were used as received without further purification.

Preparation of CH₃NH₃I

CH₃NH₃I was synthesized by the reaction of methylamine and HI with the molar ratio of 1: 1. 30 mL of methylamine (33% in methyl alcohol) was cooled to 0°C with continuous stirring, and the HI was added slowly. After stirring for 2 h, the precipitate was obtained by rotary evaporation at 60°C, followed by washing and centrifuging with diethyl ether three times, and then dried under vacuum.

Preparation of the PMMA solution

For dip coating of CH₃NH₃PbI₃, three different concentrations of PMMA were used to form a more uniform film. A stock solution of 10mg/mL PMMA was prepared by dissolving the PMMA in N,N-dimethyl formamide (DMF) and shaking for 12 hours. PMMA with concentrations ranging from 1–5mg/mL were prepared from the stock solution by diluting it with DMF and shaking. After 12 hours, all the PMMA solid particles were dissolved to form a transparent solution.

Preparation of the CH₃NH₃PbI₃-PMMA film

Equimolar quantities of CH₃NH₃I and PbI₂ at 0.2mol/L were added into PMMA DMF solution to form stoichiometric CH₃NH₃PbI₃ precursor solutions. With the mechanical vibration process, all the CH₃NH₃I and the PbI₂ were dispersed homogeneously in the PMMA-DMF solution. Then, the resultant mixture was used to dip-coat on a clear CaF₂ wafer (diameter = 1.5 mm) to form the CH₃NH₃PbI₃-PMMA film. For comparison purpose, the CH₃NH₃PbI₃ film was also prepared following the same method.

SEIRA of trinitrophenol on the CH₃NH₃PbI₃-PMMA film

A 100μL volume of TNP toluene solution (4.4 mmol/L) was dropped onto the CH₃NH₃PbI₃ and the CH₃NH₃PbI₃-PMMA films and dried in 100°C to remove the solvent. The TNP molecules on the blank substrate was also detected by the same method mentioned above.

Detections of nitroaromatic analytes

A 100μL volume of nitroaromatics molecules toluene solution (0.44 mmol/L and 4.4 mmol/L), involving TNP, PNP, DNT and PNT, were dropped onto CH₃NH₃PbI₃-PMMA film and dried in 100°C, respectively. For comparison

purpose, the nitroaromatic molecules were also detected on the blank substrate by the same method mentioned above.

Stability of CH₃NH₃PbI₃-PMMA film

The UV-vis absorption spectra of the unencapsulated CH₃NH₃PbI₃ and CH₃NH₃PbI₃-PMMA films were measured under ambient conditions with controlled humidity along with the storage time. The UV-vis absorption intensity of both films were calculated to compare the stability of the CH₃NH₃PbI₃-PMMA film with the CH₃NH₃PbI₃ film.

Characterization

Powder X-ray diffraction (XRD) patterns were performed on a Jordan Valley EX-Calibur X-ray Diffractometer at 40 kV and 35 mA using Cu K α radiation, as shown in Figure S1. The morphologies were investigated using a JEOL JSM-7800F (Japan) Scanning Electron Microscopy (SEM), as shown in Figure S2. Photoluminescence (PL) measurements were performed using a Agilent, Cary eclipse (USA) in ambient conditions. Fourier transform infrared (FTIR) spectra were measured by using a Shimadzu, IRPrestige-21 (Japan). UV-vis absorption spectra were recorded on a FLA6000 (Hangzhou) spectro- photometer.

CH₃NH₃PbI₃ – PMMA films

The infrared spectra intensity of CH₃NH₃PbI₃ films obtained by different concentrations of PMMA were compared, as shown in Figure S3. Based on the experimental results, the hybrid perovskite films obtained by a multicycle dipping and simple annealing process using the precursor solutions composed of equimolar quantities of CH₃NH₃I and PbI₂ at 0.2 mol/L dispersed homogeneously in 10 mg/mL PMMA-DMF solution was used for the following experiments.

It is known that perovskite-type hybrids are easily decomposed in the presence of moisture because of the hygroscopic amine salts. This restricts the use of halide compounds for many practical applications. To investigate the stability of the CH₃NH₃PbI₃ and CH₃NH₃PbI₃-PMMA films, the UV-vis absorption spectra of the unencapsulated film were measured under ambient conditions with controlled humidity along with the storage time, as shown in Figure S4. It was demonstrated that the existence of PMMA in the CH₃NH₃PbI₃ perovskite film supplied a good stability lasting for 15 days under a humid environment (75% humidity).

SEIRA of nitroaromatic molecules on the hybrid perovskite

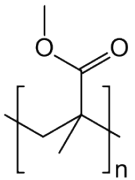
More quantitative analyses were performed to measure the changes in infrared absorption intensity at various analyte amounts to determine both the limit of detection as well as the range of linearity. Figure S6 shows the amount-dependent SEIRA intensity plotted as a function of various analyte amounts. The resulted plots exhibited a good linear relationship in the range of 0.25 nmol/mm² - 2.5 nmol/mm². This plot clearly described a linear response and was used to estimate the limit of detection (LOD) on the perovskite surface. The parameter of the linear regression of the plots and the estimated LOD was listed in Table S2 (average noise value of CH₃NH₃PbI₃-PMMA film substrate = 0.0008, LOD = 3 average blank noise / slope).

We focus on the change in the IR spectrum upon dropping nitroaromatic analytes toluene solution on the CH₃NH₃PbI₃-PMMA thin film and dried to remove the solvent. Figure S7a shows the IR spectra of a CH₃NH₃PbI₃-PMMA thin film on a CaF₂ substrate and right after dropping TNP toluene solution on the film and dried in 100°C for 1h. The peak in the spectrum around 1575 cm⁻¹ is assigned to N-H bending vibration of CH₃NH₃PbI₃. Upon dropping TNP toluene solution and dried, the IR peak positions in spectrum changes: the strength of the N-H vibration increases and the peak of N-H bending vibration shift to higher frequencies (from 1573 cm⁻¹ to 1575 cm⁻¹). The changes in the IR spectrum of TNP, p-nitrophenol (PNP), dinitrotoluene (DNT), paranitrotoluene (PNT) after

adsorbed onto $\text{CH}_3\text{NH}_3\text{PbI}_3$ -PMMA surface are also shown in Figure S7b-7e. In the experimental spectra of TNP and PNP, the peaks around 1100 cm^{-1} is clearly attributed to C-N stretch vibration, which shift to lower frequencies when TNP or PNP are adsorbed onto $\text{CH}_3\text{NH}_3\text{PbI}_3$ -PMMA surface. Also in the IR spectrum of DNT and PNT, a shift to higher frequencies for the peak assigned to aromatic nitro symmetric stretching vibration around 1345 cm^{-1} is apparent. Thus, we can draw an important conclusion that the nitroaromatic molecules are not just physical adsorbed on the $\text{CH}_3\text{NH}_3\text{PbI}_3$ surface. The change in the IR spectrum occurred by a specific chemical interaction between nitroaromatic molecules and the material as mere surface physical adsorption would not cause the change of the C-H stretch vibration and the aromatic nitro symmetric stretching vibration.

Table S1. Selection of the characteristic peaks of nitroaromatic analytes.

(a) Characteristic peaks of perovskite and PMMA.

chemical structure	infrared peak	mode assignment
Perovskite $\text{CH}_3\text{NH}_3\text{PbI}_3$	907	$\delta^t(\text{NH}_2)$ twisting vibration
	1466	$\delta(\text{C-H})$ bending vibration
	1575	$\delta(\text{N-H})$ bending vibration
	2853	$\nu^s(\text{C-H})$ symmetric stretching vibration
	2924	$\nu^{\text{as}}(\text{C-H})$ asymmetric stretching vibration
	3127	$\nu^s(\text{N-H})$ symmetric stretching vibration
	3171	$\nu^{\text{as}}(\text{N-H})$ asymmetric stretching vibration
PMMA 	1152	$\nu(\text{C-O})$ stretching vibration
	1197	$\nu^{\text{as}}(\text{C-O-C})$ asymmetric stretching vibration
	1247	$\nu^s(\text{C-O-C})$ symmetric stretching vibration
	1274	$\delta^t(\text{CH}_3)$ twisting vibration
	1367	$\delta^s(\text{CH}_3)$ symmetric deformation vibration
	1388	$\nu^s(-\text{COO})$ symmetric stretching vibration
	1450	$\delta^{\text{as}}(\text{CH}_3)$ asymmetric deformation vibration
	1487	$\delta(\text{CH}_2)$ deformation vibration
	1731	$\nu(\text{C=O})$ stretching vibration
	2954	$\nu^{\text{as}}(\text{C-H})$ asymmetric stretching vibration
	2999	$\nu^{\text{as}}(\text{CH}_3)$ asymmetric stretching vibration

(b) Selection of the characteristic peaks of nitroaromatic analytes in order to distinguish from the peaks of $\text{CH}_3\text{NH}_3\text{PbI}_3$ -PMMA film.

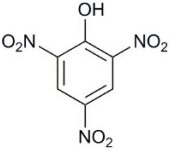
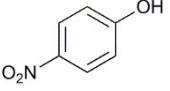
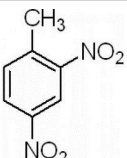
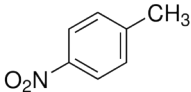
chemical structure	infrared peak	peak assignment
<p>TNP</p> 	<p>1320 1345 1546 1608 1634 3100</p>	<p>$\nu(\text{C-O})$ stretching vibration $\nu_s(\text{NO}_2)$ symmetric stretching vibration $\nu(\text{C=C})$ aromatic ring skeleton stretching $\nu(\text{C=C})$ aromatic ring skeleton stretching $\nu(\text{C=C})$ aromatic ring skeleton stretching $\nu(\text{OH})$ skeleton stretching</p>
<p>PNP</p> 	<p>1342 1488 1499 1594 1613 3424</p>	<p>$\nu^s(\text{NO}_2)$ symmetric stretching vibration $\nu(\text{C=C})$ aromatic ring skeleton stretching $\nu(\text{C=C})$ aromatic ring skeleton stretching $\nu(\text{C=C})$ aromatic ring skeleton stretching $\nu(\text{C=C})$ aromatic ring skeleton stretching $\nu(\text{OH})$ skeleton stretching</p>
<p>DNT</p> 	<p>1349 1530 1605 3103</p>	<p>$\nu^s(\text{NO}_2)$ symmetric stretching vibration $\nu(\text{C=C})$ aromatic ring skeleton stretching $\nu(\text{C=C})$ aromatic ring skeleton stretching $\nu(\text{C-H})$ stretching vibration</p>
<p>PNT</p> 	<p>1320 1345 1509 1539 1610</p>	<p>$\nu^s(\text{NO}_2)$ symmetric stretching vibration $\nu(\text{C=C})$ aromatic ring skeleton stretching $\nu(\text{C=C})$ aromatic ring skeleton stretching $\nu(\text{C=C})$ aromatic ring skeleton stretching $\nu(\text{C=C})$ aromatic ring skeleton stretching</p>

Table S2. Parameter of the linear regression and the limit of detection.

	Intercept	Slope	Adj. R-Square	LOD (nmol/mm ²)
TNP	0.01562	0.01934	0.96478	0.12
PNP	0.02549	0.0317	0.99279	0.08
DNT	0.00888	0.0287	0.99093	0.08
PNT	0.00116	0.01519	0.98073	0.16

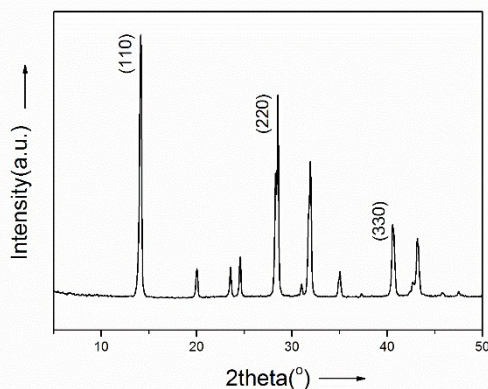


Figure S1. XRD patterns of the as-prepared $\text{CH}_3\text{NH}_3\text{PbI}_3$ film.

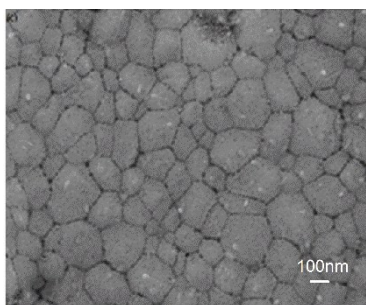


Figure S2. SEM images of the $\text{CH}_3\text{NH}_3\text{PbI}_3$ film obtained by dip-coating precursor solutions on a clear CaF_2 wafer.

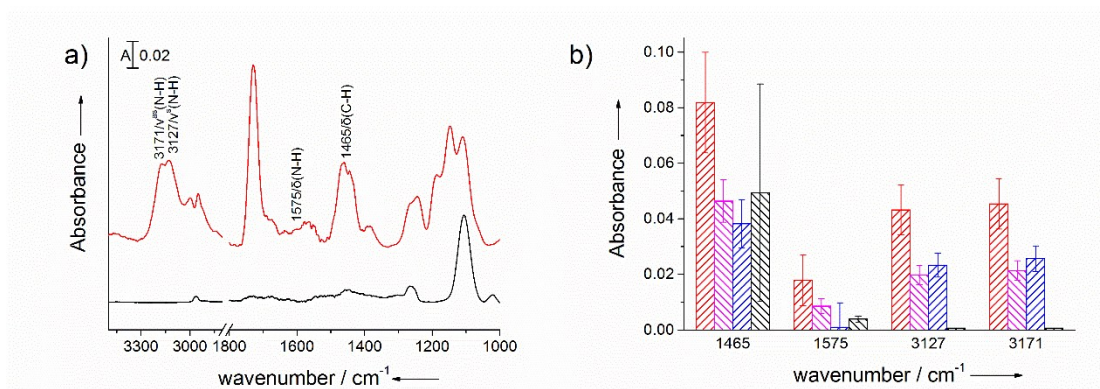


Figure S3. Infrared characterization of $\text{CH}_3\text{NH}_3\text{PbI}_3$ with the thin film obtained by different concentrations of PMMA. a) IR spectrum of the $\text{CH}_3\text{NH}_3\text{PbI}_3$ (black curve) and the $\text{CH}_3\text{NH}_3\text{PbI}_3$ -PMMA films (red curve). b) Peak heights of IR characteristic modes of the thin film without PMMA (black curve) and with different concentrations of PMMA: 10mg/mL (red curve), 5 mg/mL (purple curve), 1mg/mL (blue curve).

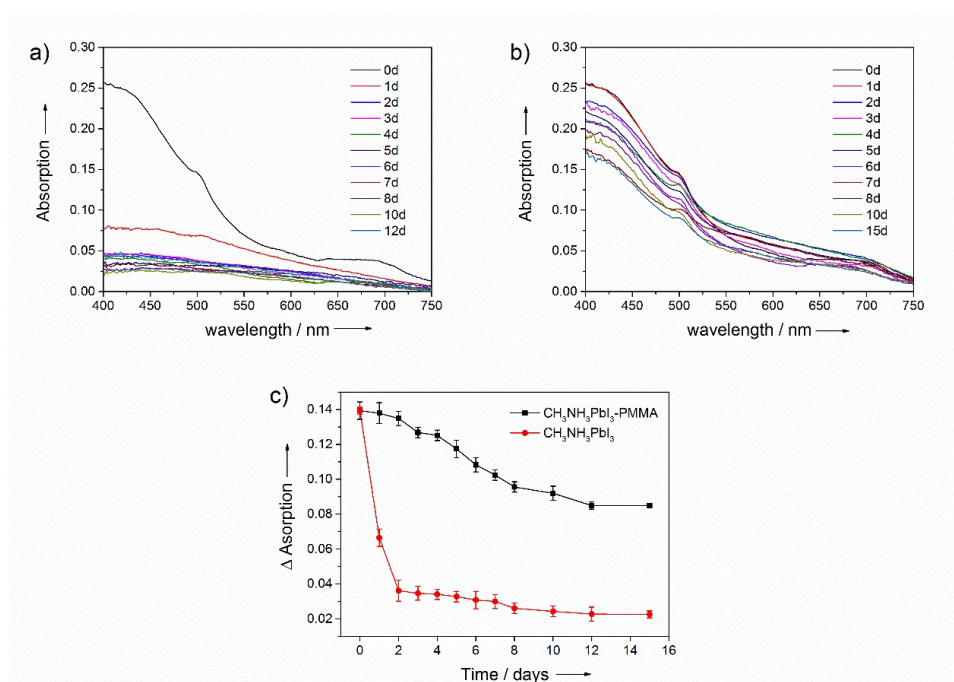


Figure S4. UV-vis absorption variation of the $\text{CH}_3\text{NH}_3\text{PbI}_3$ and $\text{CH}_3\text{NH}_3\text{PbI}_3$ -PMMA films with time stored in air at room temperature without encapsulation. The films were exposed to a humidity of 75% for consecutive days to investigate performance variation at high humidity. a) UV-vis absorption spectrum measured under exposure to ambient conditions: a) $\text{CH}_3\text{NH}_3\text{PbI}_3$ film and b) $\text{CH}_3\text{NH}_3\text{PbI}_3$ -PMMA film. c) UV-vis absorption intensity of the peak around 500nm calculated on the basis of the experimental spectra.

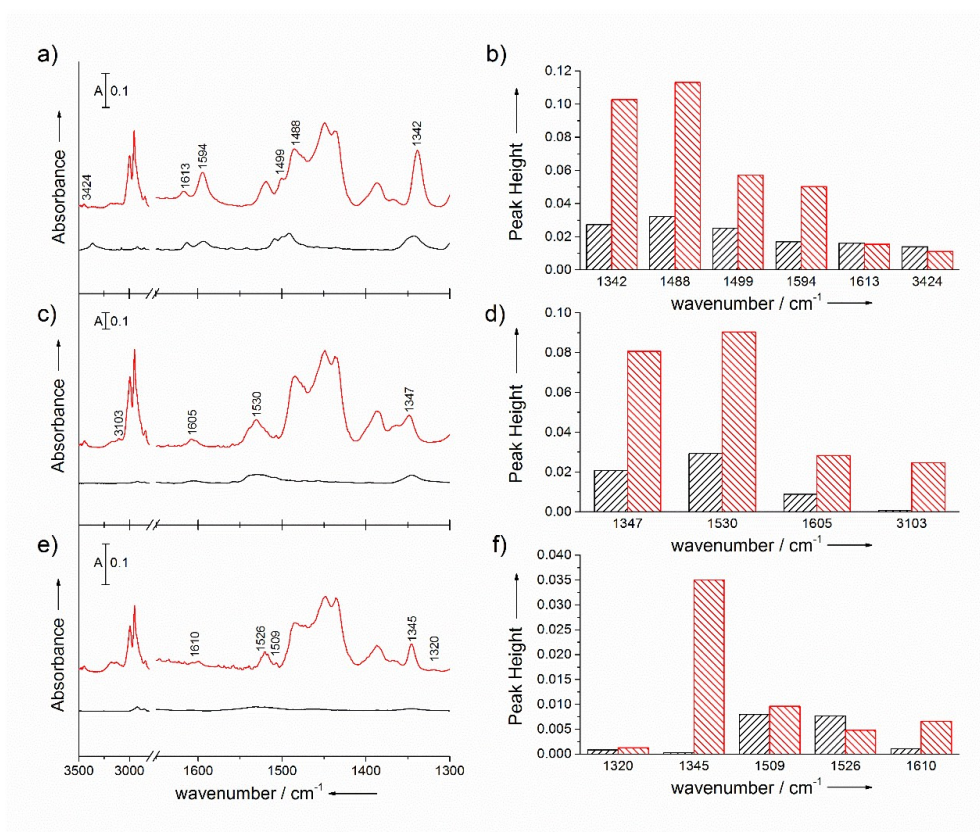


Figure S5. IR detection of a higher amount (2.5 nmol/mm^2) of nitroaromatic molecules. (a,b) TNP, (c,d) PNP, (e,f) DNT, (g,h) PNT. Left: IR spectra of the analytes on the blank substrate (black curves) and the $\text{CH}_3\text{NH}_3\text{PbI}_3$ -PMMA film substrate (red curves). Right: peak heights of characteristic IR modes of the analytes on the different substrates of the blank (black columns) and the $\text{CH}_3\text{NH}_3\text{PbI}_3$ -PMMA film (red columns).

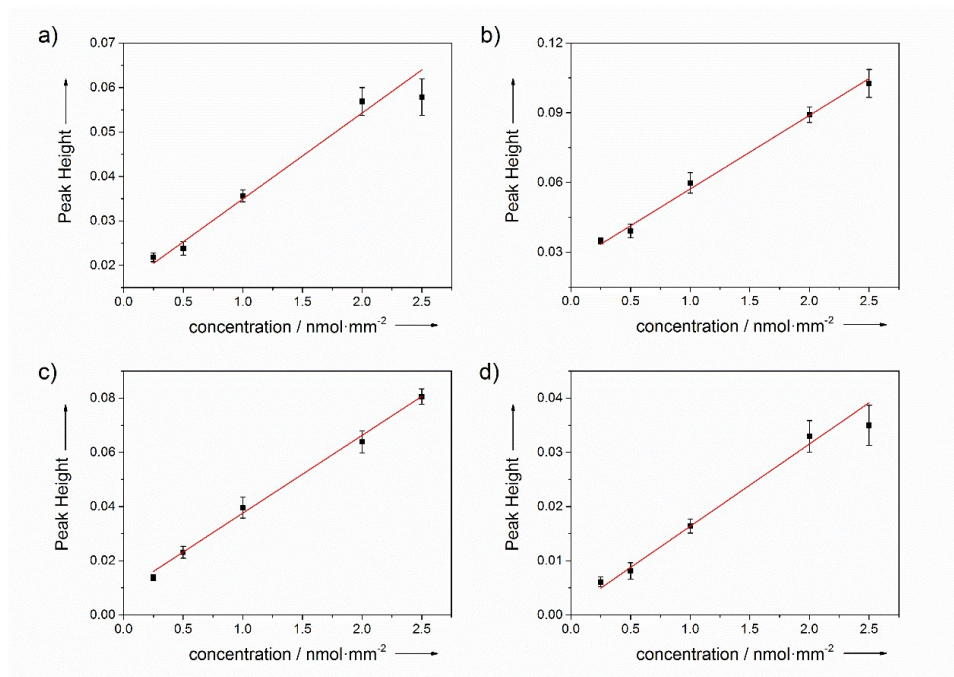


Figure S6. Infrared absorption intensity response to various analyte concentrations. a) TNP, (b) PNP, (c) DNT, (d) PNT. The peak around 1345cm⁻¹ is selected for analysis.

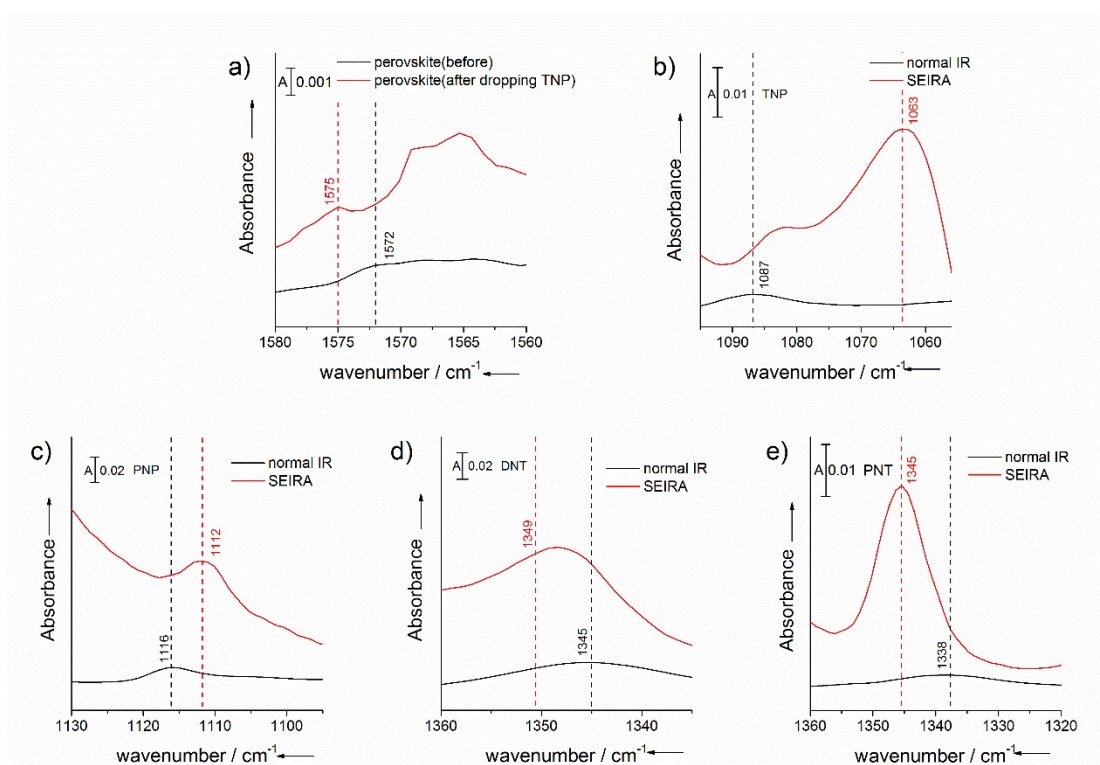


Figure S7. The change in the IR spectrum. Dashed lines mark the positions of the vibrations. a) IR spectra of CH₃NH₃PbI₃-PMMA thin film on a CaF₂ substrate and right after dropping TNP toluene solution on the film and dried in 100°C for 1h. b)c)d)e) normal IR spectrum of pure 2.5 nmol/mm² nitroaromatic analytes and SEIRA spectrum of 2.5 nmol/mm² analytes on the CH₃NH₃PbI₃-PMMA film structure: TNP(b),PNP(c),DNT(d),PNT(e).